ISBN 82-553- 0325-1
Applied Mathematics
No 2 - September 12 1977

NONLINEAR THERMAL CONVECTION IN ANISOTROPIC POROUS MEDIA

by

Oddmund Kvernvold and Peder A. Tyvand
Oslo

PREPRINT SERIES - Matematisk institutt, Universitetet i Oslo

NONLINEAR THERMAL CONVECTION IN ANISOTROPIC POROUS MEDIA

Oddmund Kvernvold and Peder A. Tyvand
Department of Mechanics
University of Oslo
Oslo, Norway

Abstract

In this paper a theoretical investigation of convection currents in anisotropic porous media is performed. The porous layer is homogeneous and bounded by two infinite, perfectly heatconducting horizontal planes. The criterion for the onset of convection is derived. The supercritical, steady two-dimensional motion, the heat transport and the stability of the motion are investigated. The results may be applied in insulation technique.

NOMENCLATURE

c_p, specific heat at constant pressure;

$\mathscr{D}$, dimensionless tensor of effective thermal diffusivity;

∇, $= (\frac{\partial}{\partial x}, \frac{\partial}{\partial y}, \frac{\partial}{\partial z})$;

∇_1^2, $= \frac{\partial^2}{\partial x^2} + \frac{\partial^2}{\partial y^2}$;

g, acceleration due to gravity;

H, heat flux;

h, thickness of porous layer;

$\vec{i}, \vec{j}, \vec{k}$, unit vectors;

$\mathscr{K}$, dimensionless permeability tensor;

K, permeability;

N, truncation parameter;

Nu, Nusselt number;

p, dimensionless pressure;

R, Rayleigh number $K_3 g \gamma \Delta T h / \kappa_{m3} \nu$;

R_0, Rayleigh number for the onset of convection;

T, dimensionless temperature;

T_0, reference temperature;

ΔT, temperature difference between lower and upper plane;

$\vec{v} = (u,v,w)$, dimensionless velocity vector;

x,y,z, dimensionless Cartesian coordinates;

Greek letters

γ, coefficient of thermal volume expansion;

$\eta_{1,2}$, thermal anisotropy parameters defined by (2.8);

θ, dimensionless temperature;

κ, thermal diffusivity;

λ, thermal conductivity;

$\xi_{1,2}$, permeability anisotropy parameters defined by (2.8);

ν, kinematic viscosity;

ρ, density;

ρ_0, standard density;

Subscripts

c, critical;

f, fluid;

m, solid-fluid mixture;

x,y,z, partial derivatives;

1,2,3, tensor components in x-, y- and z-direction, respectively;

I,II, longitudinal and transverse tensor components for a transversely isotropic medium.

Superscripts

$\overline{(\ )}$, horizontal mean;

$(^*)$, transformation given by (4.1) and (4.2);

$(\ )^{(n)}$, order of series expansion;

$(\ )'$, small disturbance of the two-dimensional steady solution.

1 INTRODUCTION

Free thermal convection in porous media has received considerable interest due to its technical and geophysical applications. So far, theoretical and experimental investigations have usually been concerned with isotropic porous media. However, in many problems the porous materials are of anisotropic nature. This is the case for fibrous insulation materials, where convection currents may occur. Another important example is groundwater motion in sediments and other anisotropic rocks, especially in areas with geothermal activity.

The papers on convection in anisotropic media are rather new and not numerous. Castinel and Combarnous [1] derived the stability criterion for porous media with anisotropic permeability, and made experiments concerning the supercritical heat transport and temperature field. Ephere [2] extended the stability analysis to media with anisotropy also in thermal diffusivity, and Tyvand [3] took into account the effect of hydrodynamic dispersion caused by a uniform basic flow. Burns, Chow and Tien [4] incorporated anisotropic permeability in their study of convection in vertical slots. Their study is relevant to insulation between walls, while our present study is relevant to insulation between floors and ceilings in buildings.

Nonlinear convection in isotropic porous media was treated numerically by Elder [5], Straus [6] and Kvernvold [7], and analytically by Palm, Weber and Kvernvold [8].

In this paper the onset of convection is analysed for a more general type of anisotropic media than in [1,2]. Moreover, the effects of anisotropy on the supercritical motion and the heat

transfer is analysed. The stability of the two-dimensional steady motion is also analysed.

In the interpretation of the results we shall concentrate about transversely isotropic media. A saturated medium is defined as transversely isotropic if it has equal values of permeability and thermal diffusivity in all directions normal to a specified direction. Four typical cases of transversely isotropic media are sketched in Fig. 1.

2 GOVERNING EQUATIONS

We consider free thermal convection in a homogeneous porous layer saturated by a homogeneous fluid. The layer is bounded above and below by two infinite and impermeable perfectly heat-conducting horizontal planes. The planes are separated by a distance h and have constant temperatures T_0 and $T_0 + \Delta T$, where the lower plane is the warmer. The saturated porous medium is assumed to have coinciding principal axes of permeability and thermal diffusivity. One of these axes is directed upwards, in z-direction. The x- and y-axes are defined by the directions of the two other principal axes. See Fig. 2.

By choosing

$$h, (c_p\rho)_m h^2/\lambda_{m3}, \kappa_{m3}/h, \Delta T, \rho_0 \nu \kappa_{m3}/K_3 \qquad (2.1)$$

as units for length, time, velocity, temperature and pressure, respectively, the governing equations in dimensionless form may be written (Bear [9], Katto and Masuoka [10])

$$\vec{v} + \mathcal{K} \cdot (\nabla p - RT\vec{k}) = 0 \qquad (2.2)$$

$$\nabla \cdot \vec{v} = 0 \qquad (2.3)$$

$$\frac{\partial T}{\partial t} + \vec{v}\cdot\nabla T = \nabla\cdot(\mathscr{D}\cdot\nabla T) \tag{2.4}$$

Here Darcy's law and the Boussinesq approximation are utilized, and the density is assumed to be a linear function of the temperature. R is the Rayleigh number defined as

$$R = \frac{K_3 g\gamma \Delta T h}{\kappa_{m3}\nu} \tag{2.5}$$

$\mathscr{K}$ and $\mathscr{D}$ are dimensionless tensors of permeability and thermal diffusivity, respectively. They will be written

$$\mathscr{K} = \xi_1 \vec{i}\vec{i} + \xi_2 \vec{j}\vec{j} + \vec{k}\vec{k} \tag{2.6}$$

$$\mathscr{D} = \eta_1 \vec{i}\vec{i} + \eta_2 \vec{j}\vec{j} + \vec{k}\vec{k} \tag{2.7}$$

where

$$\left.\begin{aligned} &\xi_1 = K_1/K_3, \quad \xi_2 = K_2/K_3 \\ &\eta_1 = \kappa_{m1}/\kappa_{m3}, \quad \eta_2 = \kappa_{m2}/\kappa_{m3} \end{aligned}\right\} \tag{2.8}$$

By eliminating the pressure from (2.2) and substituting the field variables written as

$$\left.\begin{aligned} &T = \frac{T_0}{\Delta T} - z + \theta(x,y,z,t) \\ &\vec{v} = \vec{v}(x,y,z,t) \end{aligned}\right\} \tag{2.9}$$

into (2.2) - (2.4), we obtain the following equations

$$\left(\xi_1\frac{\partial^2}{\partial x^2} + \xi_2\frac{\partial^2}{\partial y^2} + \frac{\partial^2}{\partial z^2}\right)w = R\left(\xi_1\frac{\partial^2}{\partial x^2} + \xi_2\frac{\partial^2}{\partial y^2}\right)\theta \tag{2.10}$$

$$\nabla\cdot\vec{v} = 0 \tag{2.11}$$

$$-w + \vec{v}\cdot\nabla\theta = \left(\eta_1\frac{\partial^2}{\partial x^2} + \eta_2\frac{\partial^2}{\partial y^2} + \frac{\partial^2}{\partial z^2} - \frac{\partial}{\partial t}\right)\theta \tag{2.12}$$

The requirements of perfectly heat conducting and impermeable boundaries yield the boundary conditions

$$\theta = w = 0 \quad \text{at} \quad z = 0,1 \tag{2.13}$$

3 LINEAR THEORY

The onset of convection is given by the linear version of (2.10)-(2.13). Since the system is self-adjoint, we may put $\frac{\partial}{\partial t} = 0$. By introducing the solutions

$$\left.\begin{aligned} w &\sim \sin \pi z \; e^{i(kx+ly)} \\ \theta &\sim \sin \pi z \; e^{i(kx+ly)} \end{aligned}\right\} \tag{3.1}$$

where k and l are wave numbers in x- and y-direction, respectively, we find the Rayleigh number for the onset of convection

$$R_0 = \frac{\xi_1 k^2+\xi_2 l^2+\pi^2}{\xi_1 k^2+\xi_2 l^2} (\eta_1 k^2+\eta_2 l^2+\pi^2) \tag{3.2}$$

Minimizing (3.2) with respect to k and l, we get the critical Rayleigh number

$$R_c = \pi^2\left(\text{Min}\left\{\left(\frac{\eta_1}{\xi_1}\right)^{\frac{1}{2}}, \quad \left(\frac{\eta_2}{\xi_2}\right)^{\frac{1}{2}}\right\} + 1\right)^2 \tag{3.3}$$

Case A: When

$$\eta_1/\xi_1 < \eta_2/\xi_2 \tag{3.4}$$

the critical wave numbers are

$$k_c = \pi(\xi_1\eta_1)^{-\frac{1}{4}}, \quad l_c = 0 \tag{3.5}$$

which give rolls with axis aligned in y-direction.

Case B: When

$$\eta_1/\xi_1 > \eta_2/\xi_2 \tag{3.6}$$

the critical wave numbers are

$$k_c = 0 \ , \quad l_c = \pi(\xi_2\eta_2)^{-\frac{1}{4}} \tag{3.7}$$

which give rolls with axis aligned in x-direction.

Case C: When

$$\eta_1/\xi_1 = \eta_2/\xi_2 \tag{3.8}$$

the orientation of the rolls is undetermined. The critical wave number vector

$$\vec{k}_c = k_c\vec{i} + l_c\vec{j} \tag{3.9}$$

is constrained by the relation

$$(\xi_1\eta_1)^{\frac{1}{2}}k_c^2 + (\xi_2\eta_2)^{\frac{1}{2}}\, l_c^2 = \pi^2 \tag{3.10}$$

Included in case C is horizontal isotropy, defined by

$$\xi_1 = \xi_2 = \xi, \qquad \eta_1 = \eta_2 = \eta \tag{3.11}$$

Then

$$R_c = \pi^2\left[(\eta/\xi)^{\frac{1}{2}} + 1\right]^2 \tag{3.12}$$

$$a_c = (k_c^2+l_c^2)^{\frac{1}{2}} = \pi(\xi\eta)^{-\frac{1}{4}} \tag{3.13}$$

The results for horizontal isotropy were first obtained by Epherre [2].

4 NONLINEAR THEORY

We shall examine the motion for supercritical Rayleigh numbers. It will be useful to transform the governing equations by

$$(\overset{*}{x},\overset{*}{y},\overset{*}{z}) = \left((\xi_1\eta_1)^{-\frac{1}{4}}x,\ (\xi_2\eta_2)^{-\frac{1}{4}}y, z\right) \tag{4.1}$$

$$\overset{*}{\vec{v}} = \left((\xi_1\eta_1)^{-\frac{1}{4}}u,\ (\xi_2\eta_2)^{-\frac{1}{4}}v, w\right) \tag{4.2}$$

Then (2.10)-(2.12) transform to

$$\left[\left(\frac{\xi_1}{\eta_1}\right)^{\frac{1}{2}}\frac{\partial^2}{\partial \overset{*}{x}^2} + \left(\frac{\xi_2}{\eta_2}\right)^{\frac{1}{2}}\frac{\partial^2}{\partial \overset{*}{y}^2} + \frac{\partial^2}{\partial \overset{*}{z}^2}\right]\overset{*}{w}$$

$$= R\left[\left(\frac{\xi_1}{\eta_1}\right)^{\frac{1}{2}}\frac{\partial^2}{\partial \overset{*}{x}^2} + \left(\frac{\xi_2}{\eta_2}\right)^{\frac{1}{2}}\frac{\partial^2}{\partial \overset{*}{y}^2}\right]\theta \tag{4.3}$$

$$\overset{*}{\nabla}\cdot\overset{*}{\vec{v}} = 0 \tag{4.4}$$

$$-\overset{*}{w} + \overset{*}{\vec{v}}\cdot\overset{*}{\nabla}\theta = \left[\left(\frac{\eta_1}{\xi_1}\right)^{\frac{1}{2}}\frac{\partial^2}{\partial \overset{*}{x}^2} + \left(\frac{\eta_2}{\xi_2}\right)^{\frac{1}{2}}\frac{\partial^2}{\partial \overset{*}{y}^2} + \frac{\partial^2}{\partial \overset{*}{z}^2} - \frac{\partial}{\partial t}\right]\theta \tag{4.5}$$

with the boundary conditions

$$\overset{*}{w} = \theta = 0 \quad \text{at} \quad \overset{*}{z} = 0,1 \tag{4.6}$$

In this transformed system of equations the anisotropy parameters appear only in the ratios ξ_1/η_1 and ξ_2/η_2. Accordingly $\overset{*}{\vec{v}}$ and θ are functions of ξ_1/η_1 and ξ_2/η_2. Without loss of generality, one of the parameters in each ratio can be put equal to 1. The mathematics will be simplified if we put $\xi_1 = \xi_2 = 1$. Then the equation of motion (2.2) reduces to

$$\vec{v} + \nabla p - RT\vec{k} = 0 \tag{4.7}$$

which implies $\vec{k}\cdot\nabla\times\vec{v} = 0$. Together with $\nabla\cdot\vec{v} = 0$, this means that the velocity is a poloidal vector, given by one scalar function ψ as

$$\vec{v} = \nabla\times(\nabla\times\vec{k}\psi) = (\psi_{xz}, \psi_{yz}, -\nabla_1^2\psi) \equiv \vec{\delta}\psi \tag{4.8}$$

From (2.10) the temperature field is given by

$$\theta = -\frac{1}{R}\nabla^2\psi \tag{4.9}$$

Introducing (4.9) into the heat equation (2.12) we obtain the governing equation for ψ

$$\left[(\eta_1 \frac{\partial^2}{\partial x^2} + \eta_2 \frac{\partial^2}{\partial y^2} + \frac{\partial^2}{\partial z^2} - \frac{\partial}{\partial t})\nabla^2 - R\nabla_1^2\right]\psi = \vec{\delta}\psi \cdot \nabla\nabla^2\psi \qquad (4.10)$$

The boundary conditions (2.13) are expressed as

$$\psi = \psi_{zz} = 0 \quad \text{at} \quad z = 0,1. \qquad (4.11)$$

a) ANALYTICAL SOLUTION

Two-dimensional, stationary motion.

The motion is assumed to consist of two-dimensional rolls with orientation predicted by linear theory. We consider case A :

$$\eta_1/\xi_1 < \eta_2/\xi_2 \qquad (4.12)$$

which gives motion in the xz-plane, governed by equation (4.10)

$$\left[(\eta_1 \frac{\partial^2}{\partial x^2} + \frac{\partial^2}{\partial z^2})\nabla^2 + R \frac{\partial^2}{\partial x^2}\right]\psi = \vec{\delta}\psi \cdot \nabla\nabla^2\psi \qquad (4.13)$$

Case B, $\eta_1/\xi_1 > \eta_2/\xi_2$, is covered by replacing x by y and η_1 by η_2 in (4.13).

The equation will be solved by a method introduced by Kuo [11] and applied by Palm, Weber and Kvernvold [8]. The expansion parameter, ε, is defined by

$$\varepsilon^2 = \frac{R-R_0}{R} \qquad (4.14)$$

The solution of (4.13) is written

$$\psi = \sum_{n=1}^{\infty} \varepsilon^n \psi(n) \qquad (4.15)$$

According to (4.14) the Rayleigh number is given by

$$R = \frac{R_0}{1-\varepsilon^2} = R_0 + R_{0s}(\varepsilon^2+\varepsilon^4+ \cdots + \varepsilon^{2s}) \tag{4.16}$$

where

$$R_{0s} = R_0/(1-\varepsilon^{2s}) \tag{4.17}$$

To each order, s should be chosen so that R is given exactly by (4.16). Substituting (4.14) and (4.15) into (4.13), we obtain an equation to each power of ε:

$$L\psi^{(1)} \equiv \left[(\eta_1 \frac{\partial^2}{\partial x^2} + \frac{\partial^2}{\partial z^2})\nabla^2 + R_0 \frac{\partial^2}{\partial x^2}\right]\psi^{(1)} = 0 \tag{4.18}$$

$$L\psi^{(n)} = -R_{0s}(\psi_{xx}^{(n-2)} + \psi_{xx}^{(n-4)} + \cdots) + \sum_{m=1}^{n-1} \delta\psi^{(m)} \cdot \nabla\nabla^2\psi^{(n-m)}, \quad n \geq 2 \tag{4.19}$$

The boundary conditions are

$$\psi^{(n)} = \psi_{zz}^{(n)} = 0 \quad \text{at} \quad z = 0,1 \tag{4.20}$$

The solution of (4.18) is

$$\psi^{(1)} = A_1 \cos k x \sin \pi z \tag{4.21}$$

Following Palm et al. [7], k is chosen equal to the initially preferred wave number

$$k = \pi\eta_1^{-\frac{1}{4}} \tag{4.22}$$

so that

$$R_0 = R_c = \pi^2(\eta_1^{\frac{1}{2}} + 1)^2 \tag{4.23}$$

The solution of (4.19) may be written

$$\psi^{(n)} = A_n \cos k x \sin \pi z + \sum_{p,q}' B_{pq}^{(n)} \cos p k x \sin q \pi z \tag{4.24}$$

The amplitudes $A_1, A_2, \cdots$ are found from the solvability condition

in each order, giving

$$\left.\begin{aligned} A_1 &= \left[\frac{8}{\pi^2}\frac{R_{0s}}{R_0}\,\eta_1(\eta_1^{\frac{1}{2}}+1)\right]^{\frac{1}{2}} \\ A_3 &= \left[\frac{8}{\pi^2}\frac{R_{0s}}{R_0}\,\eta_1(\eta_1^{\frac{1}{2}}+1)\right]^{\frac{1}{2}}\left(\frac{1}{2}+\frac{1}{16}\frac{R_{0s}}{R_0}\,\frac{11\eta_1+14\eta_1^{\frac{1}{2}}+3}{\eta_1+10\eta_1^{\frac{1}{2}}+1}\right) \\ A_2 &= A_4 = 0 \end{aligned}\right\} \qquad (4.25)$$

The dimensionless heat transport is given by the Nusselt number

$$Nu = 1 - (\bar{\theta}_z)_{z=0} \qquad (4.26)$$

The transformed system of equations (4.3)-(4.6) implies that the Nusselt number is a function of ξ_1/η_1 when R/R_c is given. Accordingly, the anisotropy in permeability is incorporated by replacing η_1 by η_1/ξ_1. $Nu^{(2)}$ and $Nu^{(4)}$ denote the Nusselt number to second and fourth order, respectively.

$$Nu^{(2)} = 1 + 2\,\frac{R_{0s}}{R_0}\,\varepsilon^2 \qquad (4.27)$$

$$Nu^{(4)} = Nu^{(2)} + 2\,\frac{R_{0s}}{R_0}\left(1+\frac{1}{8}\,\frac{3\frac{\eta_1}{\xi_1}-66\left(\frac{\eta_1}{\xi_1}\right)^{\frac{1}{2}}-5}{\frac{\eta_1}{\xi_1}+10\left(\frac{\eta_1}{\xi_1}\right)^{\frac{1}{2}}+1}\,\frac{R_{0s}}{R_0}\right)\varepsilon^4 \qquad (4.28)$$

The expression for $Nu^{(2)}$ shows that all curves for Nu vs. R/R_c start with the same slope. $Nu^{(4)}$, given by (4.28) with $s = 2$, is a good approximation for $R/R_c < 2$, say. It is displayed in Fig.3 as dotted curves.

The influence of anisotropy on the Nusselt number for slightly

supercritical Rayleigh number is from (4.28) given by the function

$$f(\xi/\eta) = \frac{1}{8} \frac{3\frac{\eta}{\xi} - 66(\frac{\eta}{\xi})^{\frac{1}{2}} - 5}{\frac{\eta}{\xi} + 10(\frac{\eta}{\xi})^{\frac{1}{2}} + 1} \tag{4.29}$$

which is displayed in Fig. 4. The subscripts have been dropped in order to cover both case A and B.

b) NUMERICAL SOLUTION

Stationary problem

In order to obtain a sufficiently exact solution of the problem for larger supercritical Rayleigh numbers, we have to use numerical methods. Using Galerkin's method, we shall find stationary solutions of (4.10) and later examine the stability of these nonlinear solutions with respect to small disturbances.

The steady state solution of (4.10) subjected to the boundary conditions (4.11), consists of two-dimensional rolls. For case A we may write

$$\psi = \sum_{n,m} A_{nm} e^{inkx} \varphi_m(z) \tag{4.30}$$

where

$$\varphi_m(z) = \sin m\pi z \tag{4.31}$$

satisfies the appropriate boundary conditions. The summation in (4.30) runs through all integers $-\infty < n < \infty$ and $1 \leq m < \infty$. The symmetry of the problem implies the restriction

$$A_{nm} = A_{-nm} \tag{4.32}$$

corresponding to convection cells without tilt.

To determine the unknown amplitudes A_{nm}, we substitute (4.29) into (4.10), multiply by $e^{-pkx}\varphi_q(z)$ and average over the whole fluid layer. We then obtain an infinite set of algebraic equations for A_{nm}:

$$\left.\begin{aligned}&\big((n_1 n^2k^2 + m^2\pi^2)(n^2k^2+m^2\pi^2) - R\,n^2k^2\big)A_{nm}\\&- \tfrac{1}{2}\sum_{p,q} s_{m,q}\, A_{n-p,(m-q)s_{m,q}}\, A_{pq}(p^2\alpha^2+q^2\pi^2)(pm-qs)(n\pi p)\alpha^2\pi\\&+\tfrac{1}{2}\sum_{p,q} A_{n-p,m+q}(p^2\alpha^2+q^2\pi^2)(pm+qs)(n-p)\alpha^2\pi = 0\end{aligned}\right\} \quad (4.33)$$

where

$$s_{m,q} = \begin{cases} 1 & m > q \\ 0 & m = q \\ -1, & m < q \end{cases} \quad (4.34)$$

In order to solve this set it is necessary to truncate the series (4.33). The numerical computation shows that the series converges more rapidly with increasing n than with increasing m. Hence, we choose to neglect all terms with

$$|n| + \frac{m+1}{2} > N \quad (4.35)$$

where N is a sufficiently large number.

Because of the symmetry in the equations (4.33), the solution will only contain amplitudes with $n+m$ even, giving $N \times \frac{N+1}{2}$ equations to be solved. For a given N the algebraic equations are solved by a Newton-Raphson iteration procedure. Usually we need less than 5 iterations to obtain a satisfactory exact solution. A more serious problem, however, is the value of the truncation parameter N.

Following Busse [12], we assume the solution to be sufficiently accurate if, when replacing N by N+1, the Nusselt number varies less than 1 per cent.

The results of the numerical computations are shown in Fig. 3, 5 and 6. The wave number is always chosen so that the Nusselt number obtains its maximum for the given values of R/R_c and ξ/η. However, the variation of the Nusselt number with the wave number is very small.

Fig. 3 shows the Nusselt number vs. the supercritical Rayleigh number for selected values of anisotropy. For moderate anisotropy and moderately supercritical Rayleigh numbers the deviations from isotropy are small.

Fig. 5 is analogous to Fig. 4 and shows the Nusselt number variation with ξ/η when $R/R_c = 5.0$. Fig. 6 shows the value of ξ/η which gives minimum Nu for each choice of R/R_c. This is not of practical importance, because these minimum values are always very close to the values for isotropy.

Stability of the steady two-dimensional solution.

To examine the stability of the steady two-dimensional motion, we replace ψ by $\psi + \psi'$ in (4.10). ψ' means a small disturbance of the steady solution. The equation for ψ' is linearized, and becomes

$$\left[\left(\eta_1 \frac{\partial^2}{\partial x^2} + \eta_2 \frac{\partial^2}{\partial y^2} + \frac{\partial^2}{\partial z^2} - \frac{\partial}{\partial t}\right)\nabla^2 + R\nabla_1^2\right]\psi' \tag{4.36}$$

$$= \mathring{\delta}\psi' \cdot \nabla\nabla^2\psi + \mathring{\delta}\psi \cdot \nabla\nabla^2\psi'$$

The boundary conditions are

$$\psi' = \psi'_{zz} = 0 \quad \text{for} \quad z = 0,1 \tag{4.37}$$

If there exists a solution of (4.36) with growing time dependence, the stationary solution is said to be unstable. Otherwise it is stable.

For case I) we may write

$$\psi' = \sum_{n,m} A'_{nm}\, e^{inkx}\, e^{i(dx+by)+\sigma t}\, \varphi_m(z) \tag{4.38}$$

where b and d are free parameters.

For case II), the factor e^{inkx} must be replaced by e^{inly}.

The equations for the unknowns A'_{nm} are obtained by multiplying (4.36) by $e^{-ip\alpha x}\, e^{-i(dx+by)-\sigma t}\, \varphi_q(z)$ and averaging over the whole fluid layer. We neglect, as in the stationary case, all terms with $|n| + \frac{m+1}{2} > N$, where N has the same value as in the corresponding stationary problem. The system of linear homogeneous equations constitute an eigenvalue problem for σ. The analysis of the eigenvalue problem is simplified because it separates into two subsystems with either $n+m$ even or $n+m$ odd.

The eigenvalue is given by

$$\sigma = \sigma(k,R,b,d) \tag{4.39}$$

and for a given k and R, we have to vary both b and d to find the most critical disturbances. Fortunately, numerical results show that the most unstable perturbations occur for either $b = 0$ or $d = 0$. Disturbances with $b = 0$ have axis parallel to the axis of the stationary rolls. The corresponding instability is termed Eckhaus instability. Disturbances with $d = 0$ give instability termed cross-roll instability, when b is of the same order of magnitude as k, and zig-zag instability when $b \to 0$.

We first consider the case of horizontal isotropy, defined by (3.11). All rolls have the same linear stability, independent of orientation. In this case it turns out that cross-rolls are most unstable, except for a small domain with $k < k_c$ and R slightly supercritical where we get zig-zag instability. The transformed equations in the beginning of this chapter imply that the stability domain in the α/α_c - R/R_c-plane is a function of ξ/η. The results for two rather extreme values of ξ/η (100 and 1/100) are shown in Fig. 8. The isotropic case is also displayed as a comparison. We obtain corrections of the results given by Straus [6] and Kvernvold [7] because they overlooked the zig-zag instability. The domains of stability are within closed curves. Accordingly, there are upper limits for the Rayleigh numbers giving steady two-dimensional motion. We notice that no oscillatory instability will occur for horizontal isotropy. Values of ξ/η between these extreme values being displayed, give stability regions as intermediate cases of the displayed regions.

Let us consider media which are horizontally anisotropic. The stationary problem is principally the same as for horizontally isotropic media because the properties along the axis of the rolls have no influence on the steady motion. But there is a fundamental difference with respect to the stability of this motion. When we have horizontal anisotropy, the cross-rolls and zig-zags will be linearly stable for small supercritical Rayleigh number. The stability region is therefore determined by Eckhaus instability in a certain supercritical domain, which is larger the more ξ_1/η_1 deviates from ξ_2/η_2.

Therefore, a horizontally anisotropic medium has larger stability region than the horizontally isotropic medium with the same stationary problem.

We display only one example of stability for horizontally anisotropic media, curve II on Fig. 8, which is given by $\xi_1/\eta_1 = 10$ and $\xi_2/\eta_2 = 1$. Curve I gives the stability region for a horizontally isotropic medium with the same stationary problem. The stability domains are bounded by solid curves, indicating exponential instabilities, and one broken curve, indicating oscillatory instability. The dotted curve is the neutral curve of linear stability, which is common for both cases.

5 APPLICATIONS IN INSULATION TECHNIQUE

From the above general results we will discuss the insulation properties of transversely isotropic porous materials. Our aim is to minimize the loss of heat through a horizontal layer.

Let K_I and K_{II} denote longitudinal and transverse permeability, respectively, and κ_{mI} and κ_{mII} longitudinal and transverse effective thermal diffusivity, respectively.

In the conduction regime the heat transport is proportional to the vertical thermal diffusivity. It is therefore important to orientate the material in order to get minimum vertical diffisivity.

It is also important to delay the onset of convection, both to prevent convective heat transport and perhaps also to prevent wearing of the porous material by convection currents. For horizontal isotropy given by

$$\xi_1 = \xi_2 = K_{II}/K_I, \quad \eta_1 = \eta_2 = \kappa_{mII}/\kappa_{mI} \tag{5.1}$$

the critical temperature difference is from (3.12)

$$\Delta T_c = \frac{\nu\pi^2}{ga h}\left[\left(\frac{\kappa_{mI}}{K_I}\right)^{\frac{1}{2}} + \left(\frac{\kappa_{mII}}{K_{II}}\right)^{\frac{1}{2}}\right]^2 \tag{5.2}$$

When the material is turned 90° we get, say, isotropy in the xz-plane. We then have

$$\xi_1 = K_I/K_{II}, \quad \eta_1 = \kappa_{mI}/\kappa_{mII}, \quad \xi_2 = \eta_2 = 1 \tag{5.3}$$

giving from (3.3)

$$\Delta T_c = \frac{\nu\pi^2}{ga^2h}\left[\mathrm{Min}\left\{\left(\frac{\kappa_{mI}}{K_I}\right)^{\frac{1}{2}}, \left(\frac{\kappa_{mII}}{K_{II}}\right)^{\frac{1}{2}}\right\} + \left(\frac{\kappa_{mII}}{K_{II}}\right)^{\frac{1}{2}}\right]^2 \tag{5.4}$$

The class of materials defined by

$$\kappa_{mI}/K_I > \kappa_{mII}/K_{II} \tag{5.5}$$

may appropriately be termed "parallel, perforated plates", see Fig. 1 (a) and (b). Eqs. (5.2) and (5.4) imply that horizontal plates have larger critical temperature difference than vertical plates.

The other class of materials defined by

$$\kappa_{mI}/K_I \leq \kappa_{mII}/K_{II} \tag{5.6}$$

will be termed "parallel fibres", see Fig. 1 (c) and (d). The critical temperature difference is the same for horizontal and vertical fibres.

The dimensionless heat transport after the onset of convection is measured by the Nusselt number. Fig. 3 shows that the Nusselt number dependence on R/R_c is different for different anisotropy. It is, however, the dimensional heat transport which is of importance from a physical point of view. But, because of the different effects involved in the heat transport, it is not possible to give further general conclusions.

An interesting special case is the thermally isotropic material

($\kappa_{mI} = \kappa_{mII}$). This is usually a good approximation for insulation materials. In this case we conclude:

1. Horizontal fibres always give less heat transport than the same fibres turned vertically. The critical temperature difference is the same, and the difference in heat transport is solely due to the difference in Nusselt number as given by Fig. 4 and 5.

2. For perforated plates the problem is more complicated. The Nusselt number for horizontal plates is given by the lower branch (dotted curve) in Fig. 4 and 5. It is less than the Nusselt number for vertical plates when ξ/η is small and greater when ξ/η is large. The Nusselt number for vertical plates is the same as for isotropy. The critical temperature difference is, however, higher for horizontal plates than for vertical plates, so that the total heat transport (conduction + convection) is greater for vertical plates than for horizontal plates. This is seen from Fig. 9 where we have displayed the heat flux vs. temperature difference for various values of K_I, while K_{II} and $\kappa_{mI} = \kappa_{mII}$ are constant. Curve V gives the heat flux for vertical plates, and curve VI and VII give the heat flux for two types of horizontal plates. From this figure we also conclude that the type of media giving best insulation, is horizontally isotropic media with as small vertical permeability as possible.

6 SUMMARY

A theoretical analysis of thermal convection in anisotropic porous media is performed. The criterion for the onset of convection is derived. Moreover, the supercritical steady two-dimensional motion is investigated both analytically and numerically, and the

stability region of this motion is found. The analytical results are valid for Rayleigh numbers less than 2 times the critical value R_c, and for all values of the anisotropy parameters ξ_1, ξ_2, η_1 and η_2. The numerical results, which are valid in the whole domain of stable, steady two-dimensional motion, are only given for some representative values of the anisotropy parameters.

It is shown that the Nusselt number and the stability regions are functions of the anisotropy parameters in the forms ξ_1/η_1 and ξ_2/η_2.

It is found that the steady two-dimensional motion is principally the same for horizontally anisotropic as for horizontally isotropic media. The stability regions, however, are considerably larger for the former type of media and principally different from those of horizontal isotropy.

The theory may be of interest in hydrological science and in insulation technique. The nonlinear effects of anisotropy are, however, surprisingly small compared with the linear effects known from earlier work [1,2]. Burns, Chow and Tien [4] also found small nonlinear effects of anisotropy. But their problem is so different from ours that the results cannot be compared.

ACKNOWLEDGEMENTS

The authors wish to thank Dr. M. Tveitereid and Dr. J.E. Weber for valuable discussions during the preparation of this paper.

REFERENCES

1. G. Castinel and M. Comparnous, Convection naturelle dans une couche poreuse anisotrope, Rev. Thermique 168, 937-947 (1975).

2. J.F. Epherre, Critére d'apparition de la convection naturelle dans une couche poreuse anisotrope, Rev. Thermique 168, 949-950 (1975).

3. P.A. Tyvand, Heat dispersion effect on thermal convection in anisotropic porous media, J.Hydrology 34, 335-342 (1977).

4. P.J. Burns, L.C. Chow and C.L. Tien, Convection in a vertical slot filled with porous insulation, Int.J.Heat Mass Transfer 20, 919-926 (1977).

5. J.W. Elder, Steady free convection in a porous medium, J.Fluid Mech. 27, 29-48 (1967).

6. J.M. Straus, Large amplitude convection in porous media, J.Fluid Mech. 64, 51-63 (1974).

7. O. Kvernvold, Non-linear convection in a porous medium, Inst.Math., Univ. of Oslo, Preprint Ser.No.1 (1975).

8. E.Palm, J.E.Weber and O.Kvernvold, On steady convection in a porous medium,J.Fluid Mech. 54, 153-161 (1972).

9. J.Bear, Dynamics of Fluids in Porous Media,American Elsevier, New York (1972).

10. Y.Katto and T.Masuoka, Criterion for the onset of convection in a fluid in a porous medium, Int.J.Heat Mass Transfer 10, 297-309 (1967).

11. H.L. Kuo, Solution of the non-linear equations of celluar convection and heat transport,J.Fluid Mech.10,611-634(1961).

12. F.H.Busse, On the stability of two-dimensional convection in a layer heated from below.J.Math.Phys.46, 140-150 (1967).

FIGURE LEGENDS

Fig. 1 Sketches of transversely isotropic media composed of equally spaced, parallel perforated plates or parallel fibres.
(a) Horizontal plates.
(b) Vertical plates.
(c) Vertical fibres.
(d) Horizontal fibres.

Fig. 2 General model.

Fig. 3 Nu vs. R/R_c for some choices of ξ/η.

Fig. 4 f as a function of ξ/η. The solid curve covers $0 < \xi/\eta \leq 1$ expressed by $(\xi/\eta)^{\frac{1}{2}}$ as abscissa. The dotted curve covers $1 \leq \xi/\eta < \infty$ expressed by $(\xi/\eta)^{-\frac{1}{2}}$ as abscissa.

Fig. 5 Nu as a function of ξ/η for $R/R_c = 5.0$. Abscissas as in Fig. 4.

Fig. 6 The value of ξ/η giving minimum Nu for each value of R/R_c.

Fig. 7 Stability domains for the steady two-dimensional motion in the a/a_c - R/R_c - plane, for selected values of ξ/η (horizontal isotropy).

Fig. 8 Stability domains for the steady two-dimensional motion in the k/k_c - R/R_c - plane.
I : Horizontal isotropy, $\xi/\eta = 10$.
II : $\xi_1/\eta_1 = 10$, $\xi_2/\eta_2 = 1$.
III: Neutral curve for the onset of convection.

Fig. 9 Comparison of the heat flux vs. temperature difference for different media with equal, isotropic diffusivity and K_{II} kept fixed.

I	:	K_I/K_{II} = 100,	longitudinal direction	vertically
II	:	-"- = 100,	—"—	horizontally
III	:	-"- = 10,	—"—	vertically
IV	:	-"- = 10,	—"—	horizontally
V	:	-"- $\leq$ 1,	—"—	horizontally
VI	:	-"- = 1/10,	—"—	vertically
VII	:	-"- = 1/100,	—"—	vertically

Broken curve means two-dimensional, steady motion unstable.

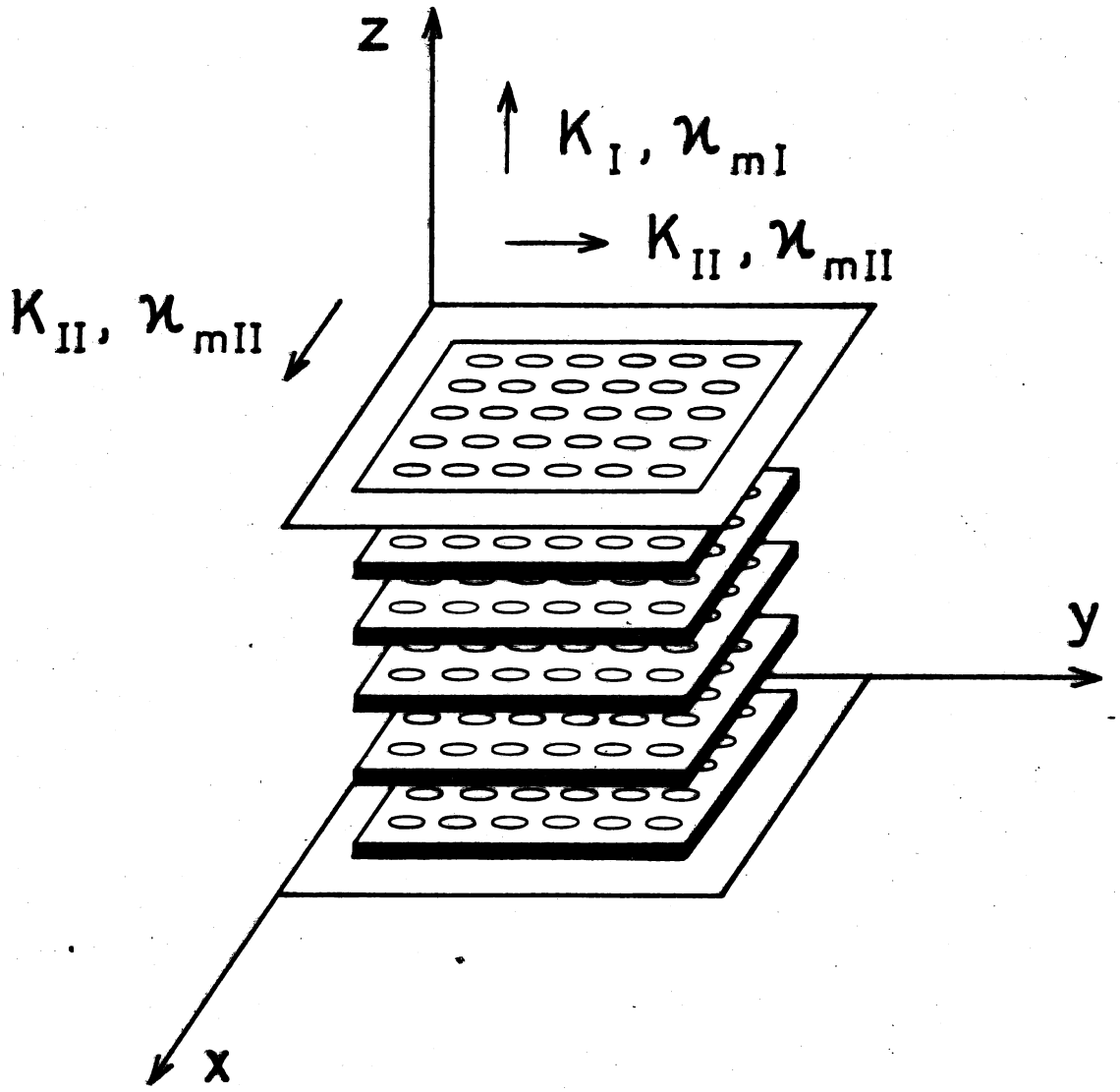

Fig. 1 (a)

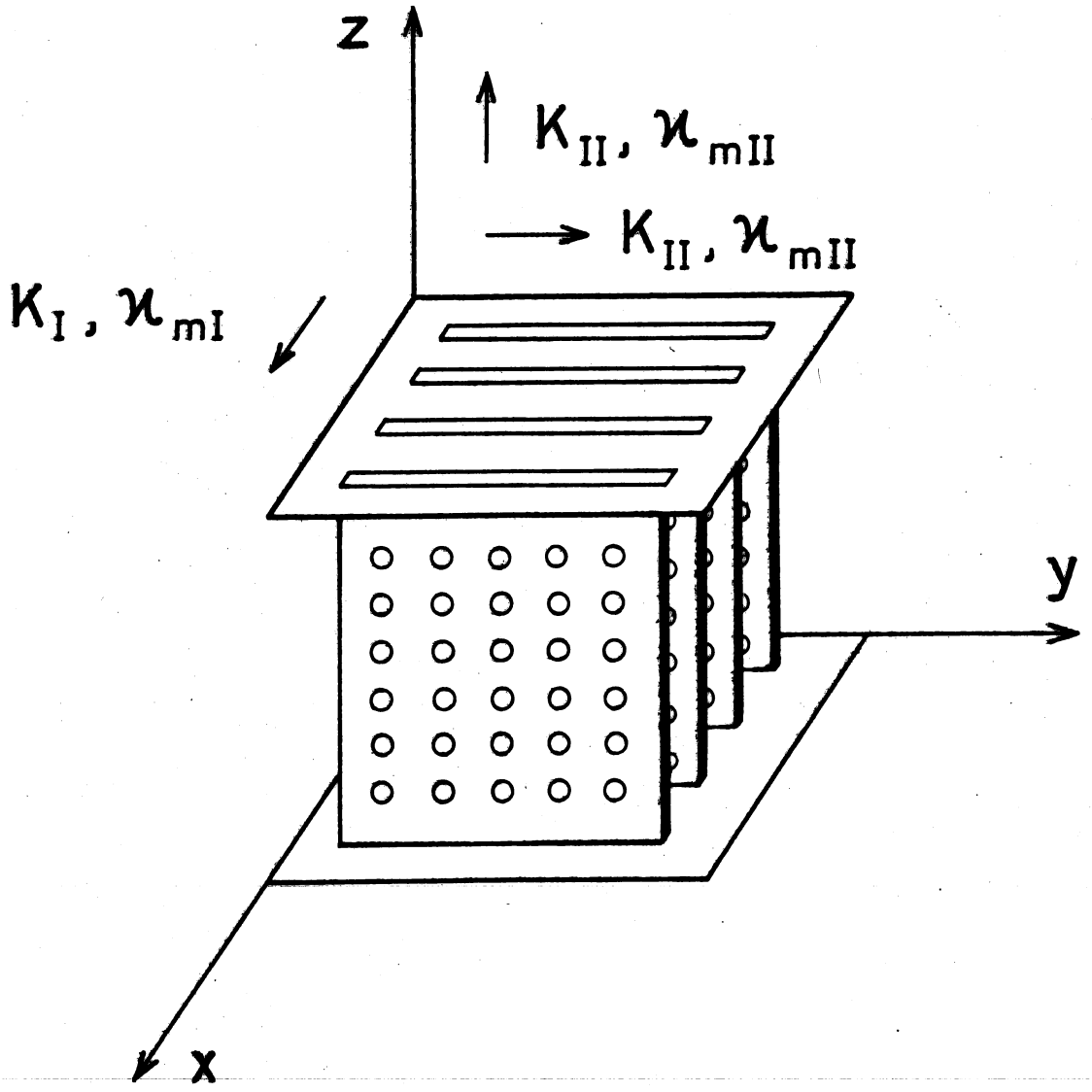

Fig. 1 (b)

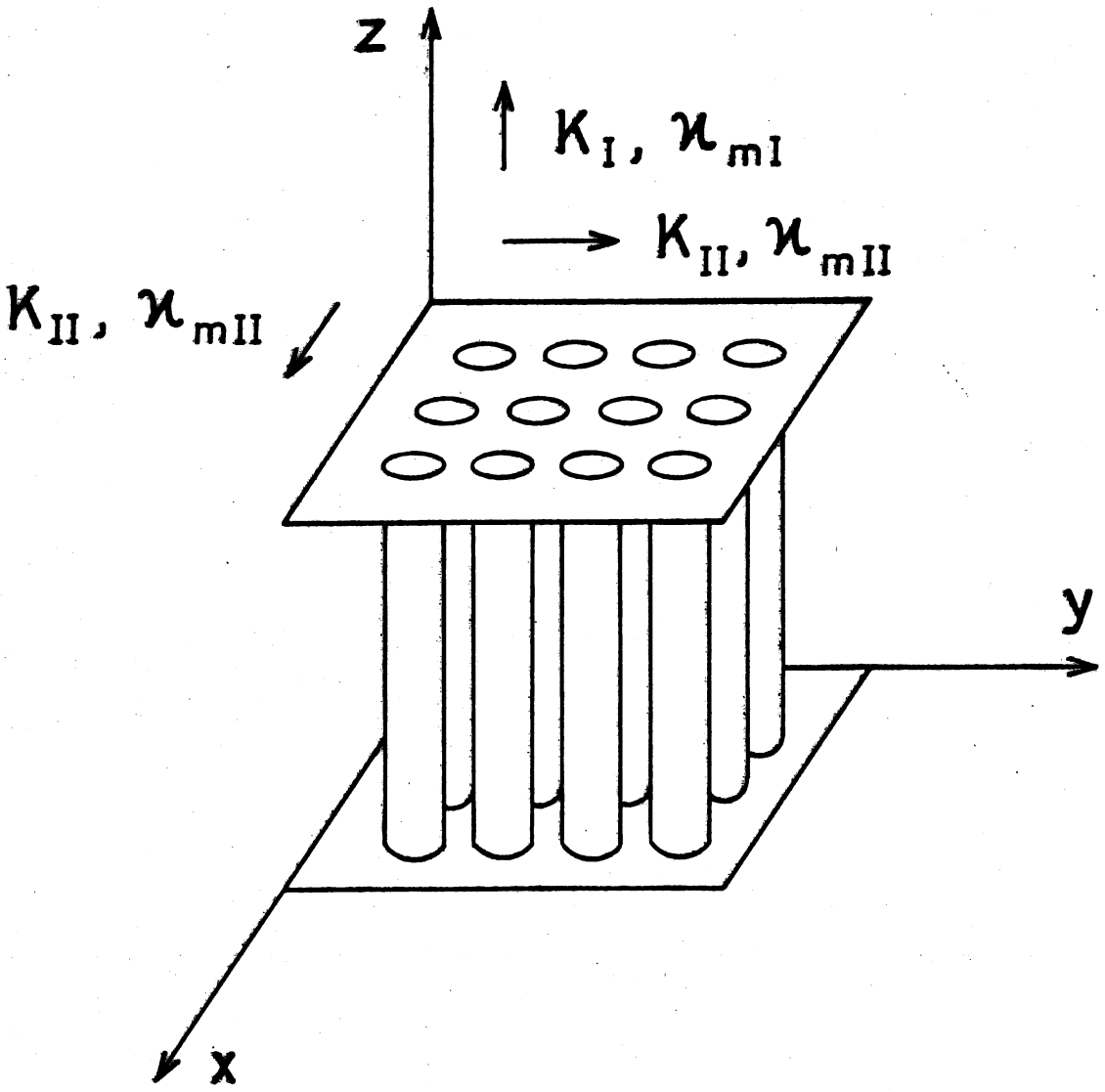

Fig. 1 (c)

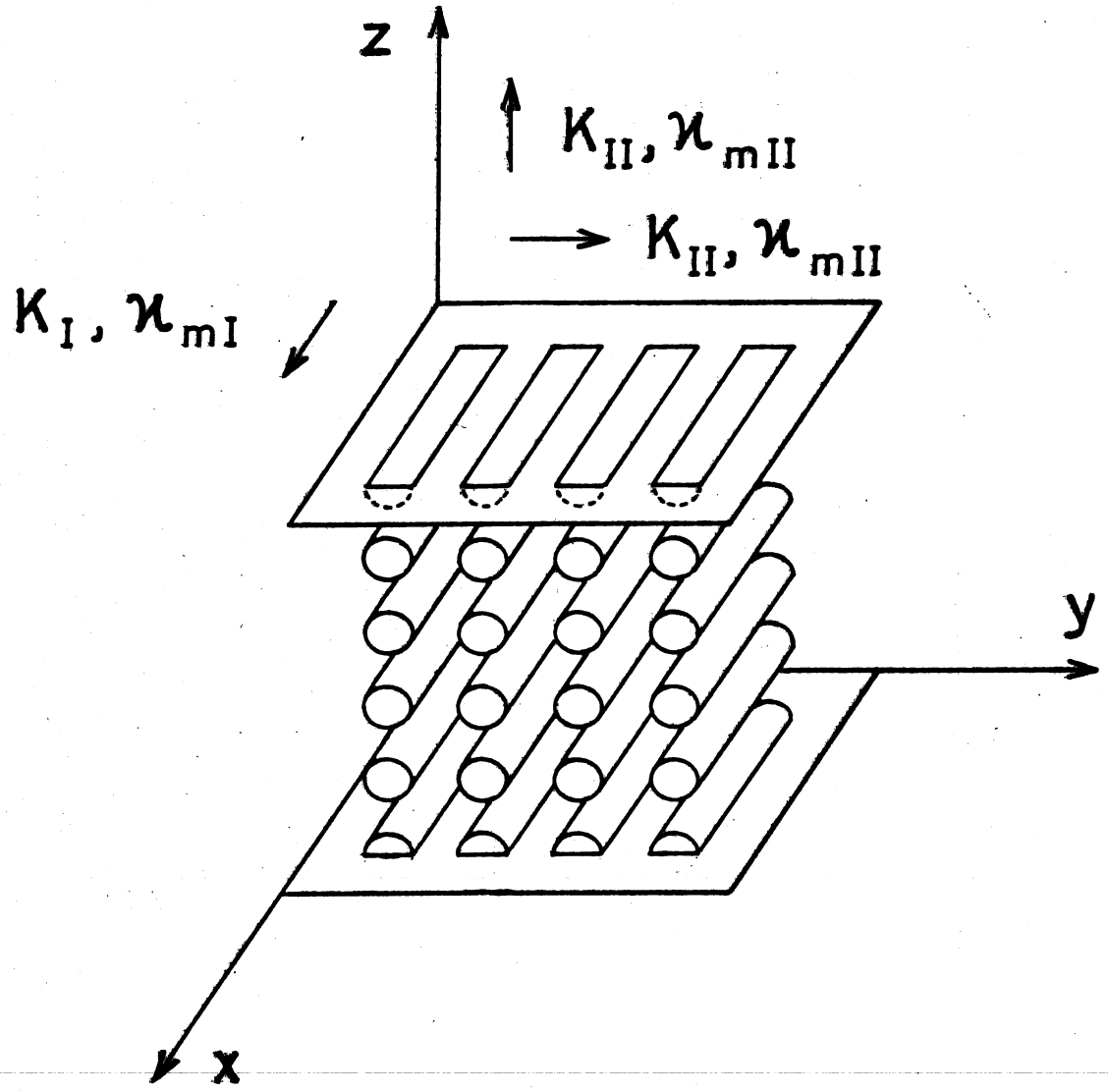

Fig. 1 (d)

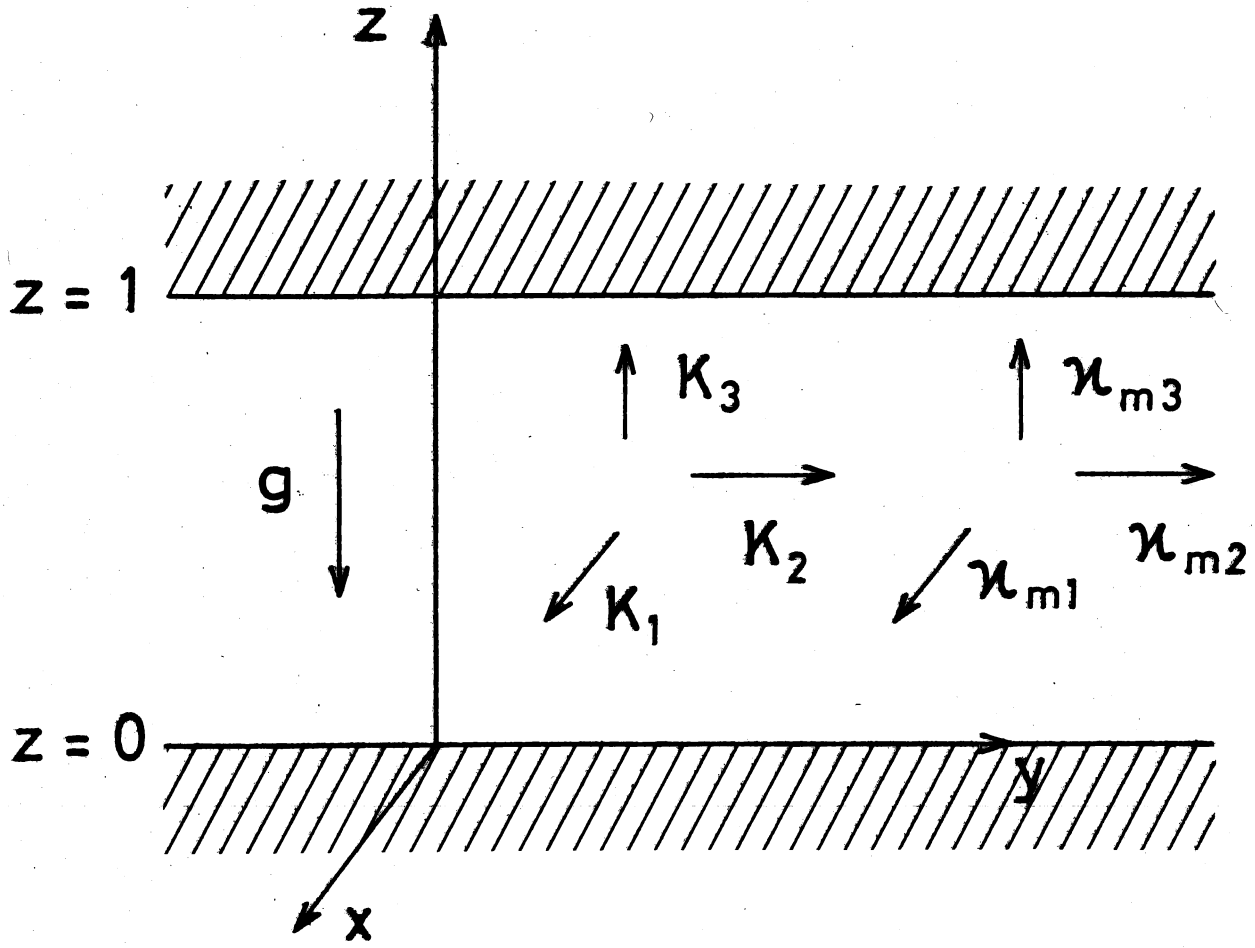

Fig. 2

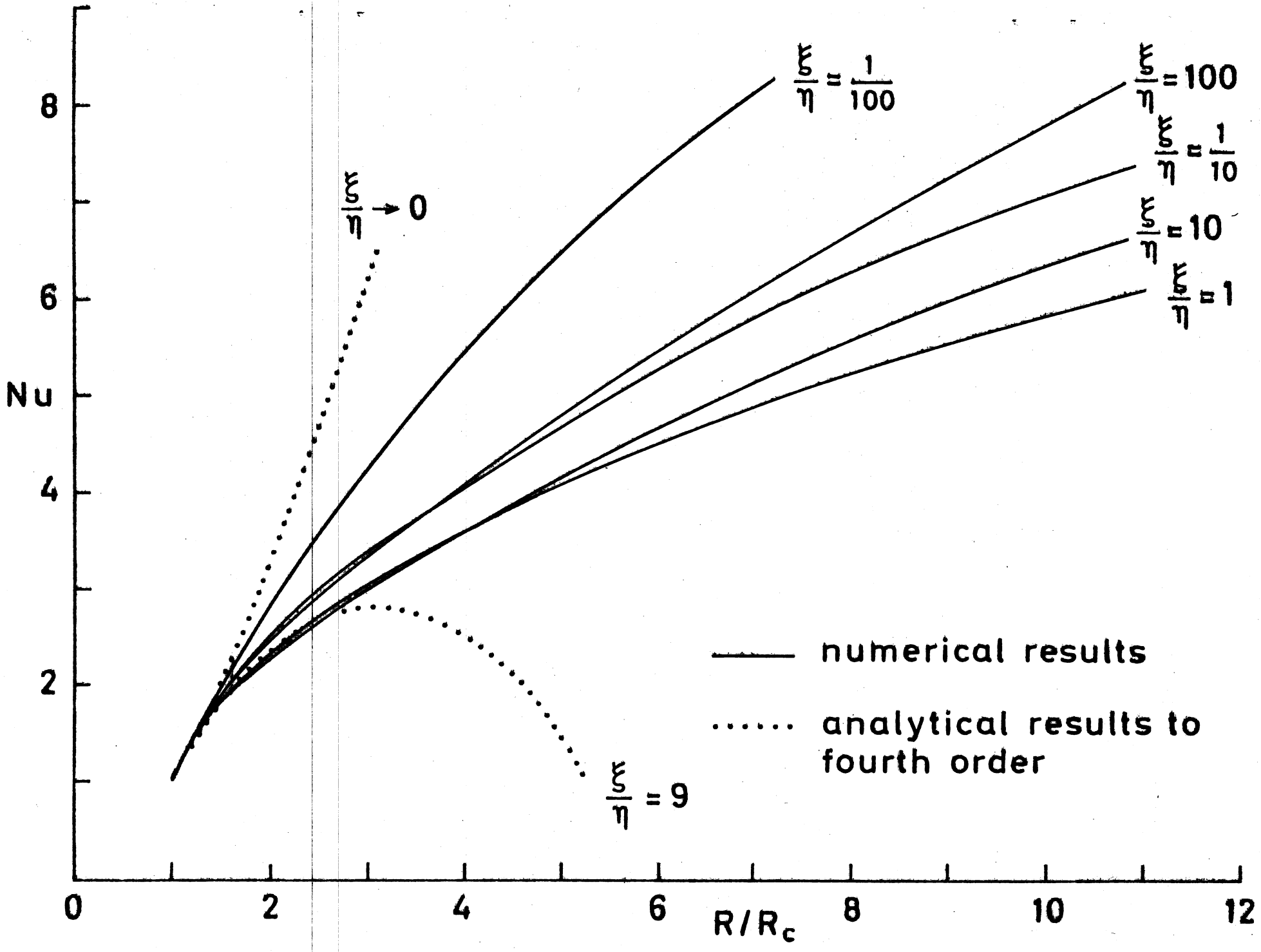
Nu
R/Rc
0
2
4
6
8
10
12
ξ/η → 0
ξ/η = 1/100
ξ/η = 100
ξ/η = 1/10
ξ/η = 10
ξ/η = 1
ξ/η = 9
numerical results
analytical results to fourth order

Fig. 3

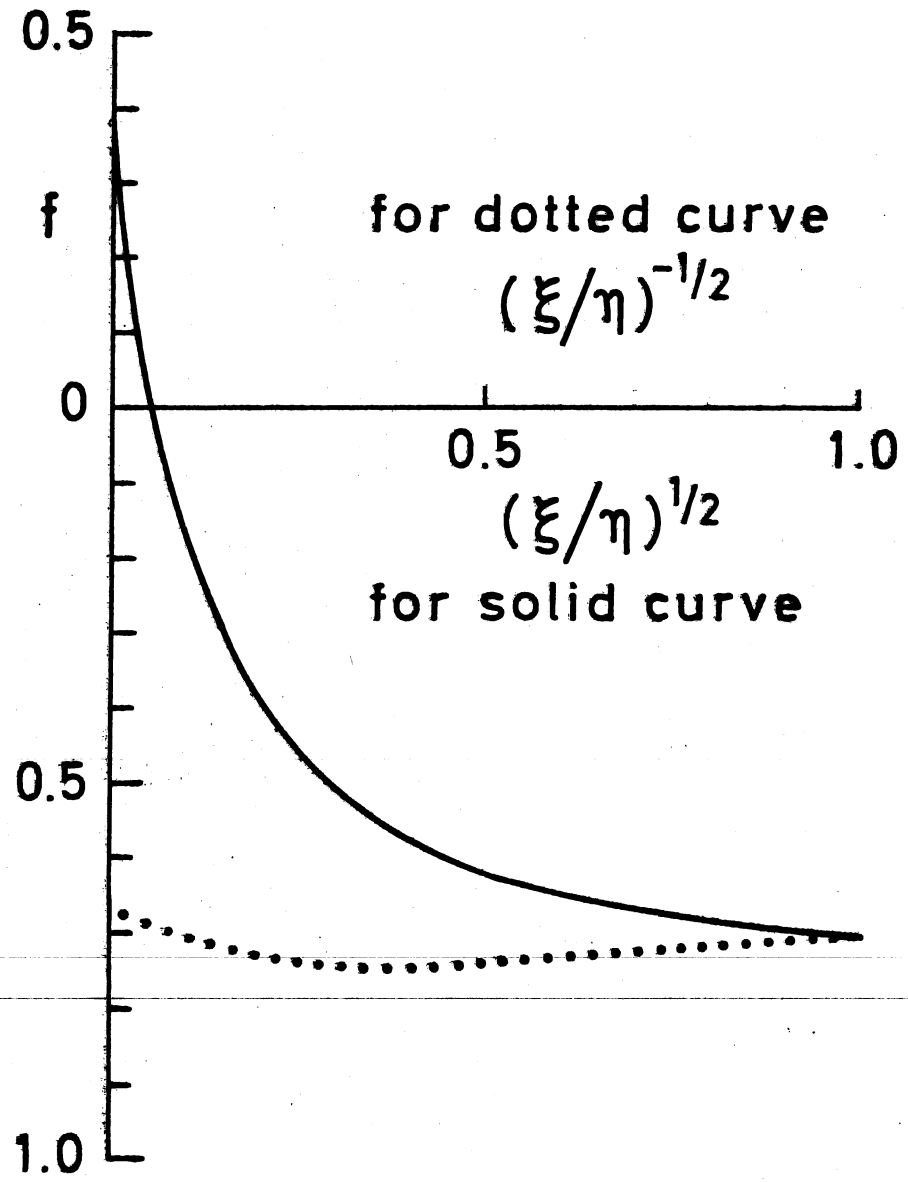
0.5
f
for dotted curve
$(\xi/\eta)^{-1/2}$
0
0.5
1.0
$(\xi/\eta)^{1/2}$
for solid curve
0.5
1.0

Fig. 4

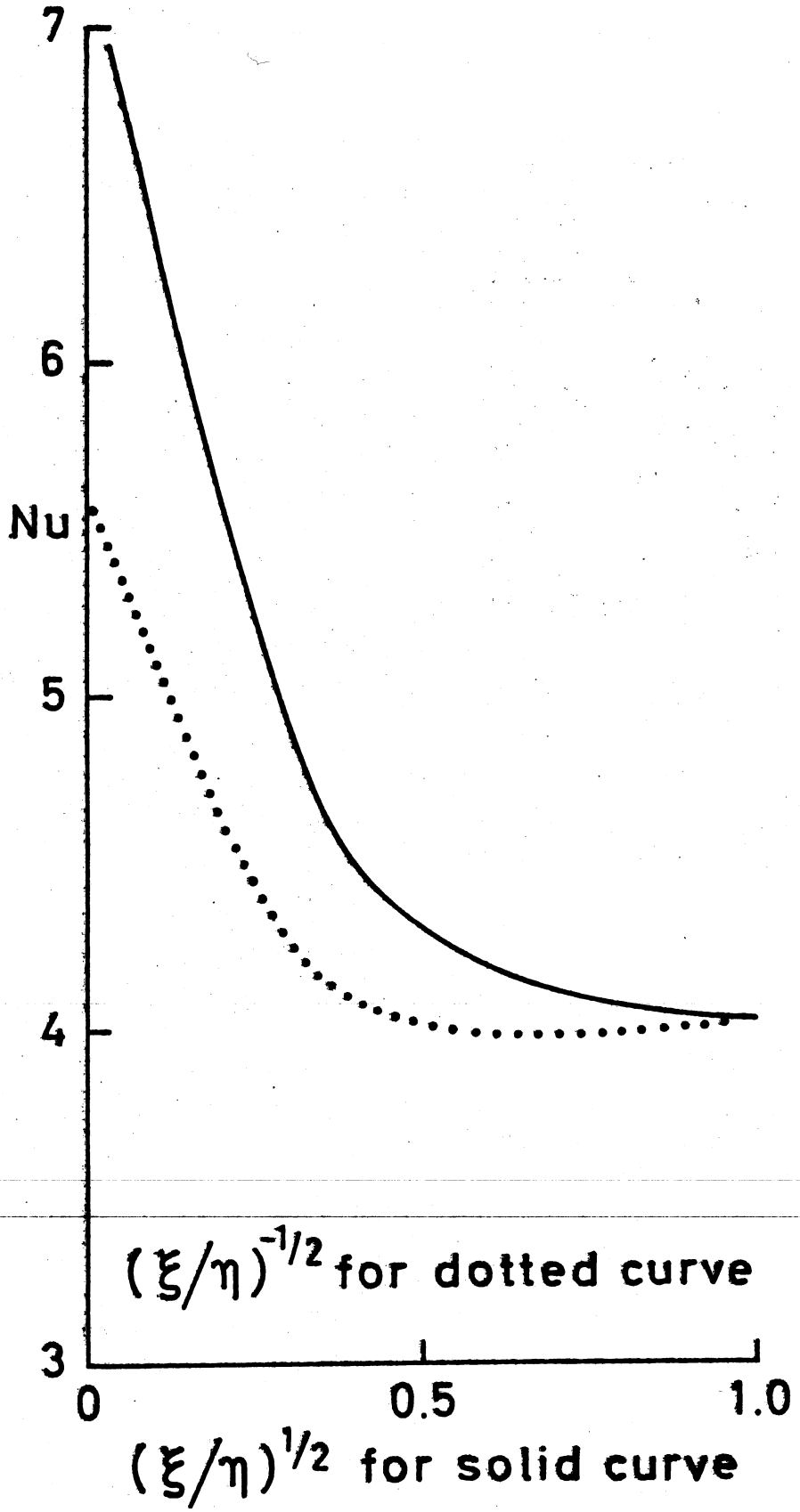
7
6
Nu
5
4
3
0
0.5
1.0
$(\xi/\eta)^{-1/2}$ for dotted curve
$(\xi/\eta)^{1/2}$ for solid curve

Fig. 5

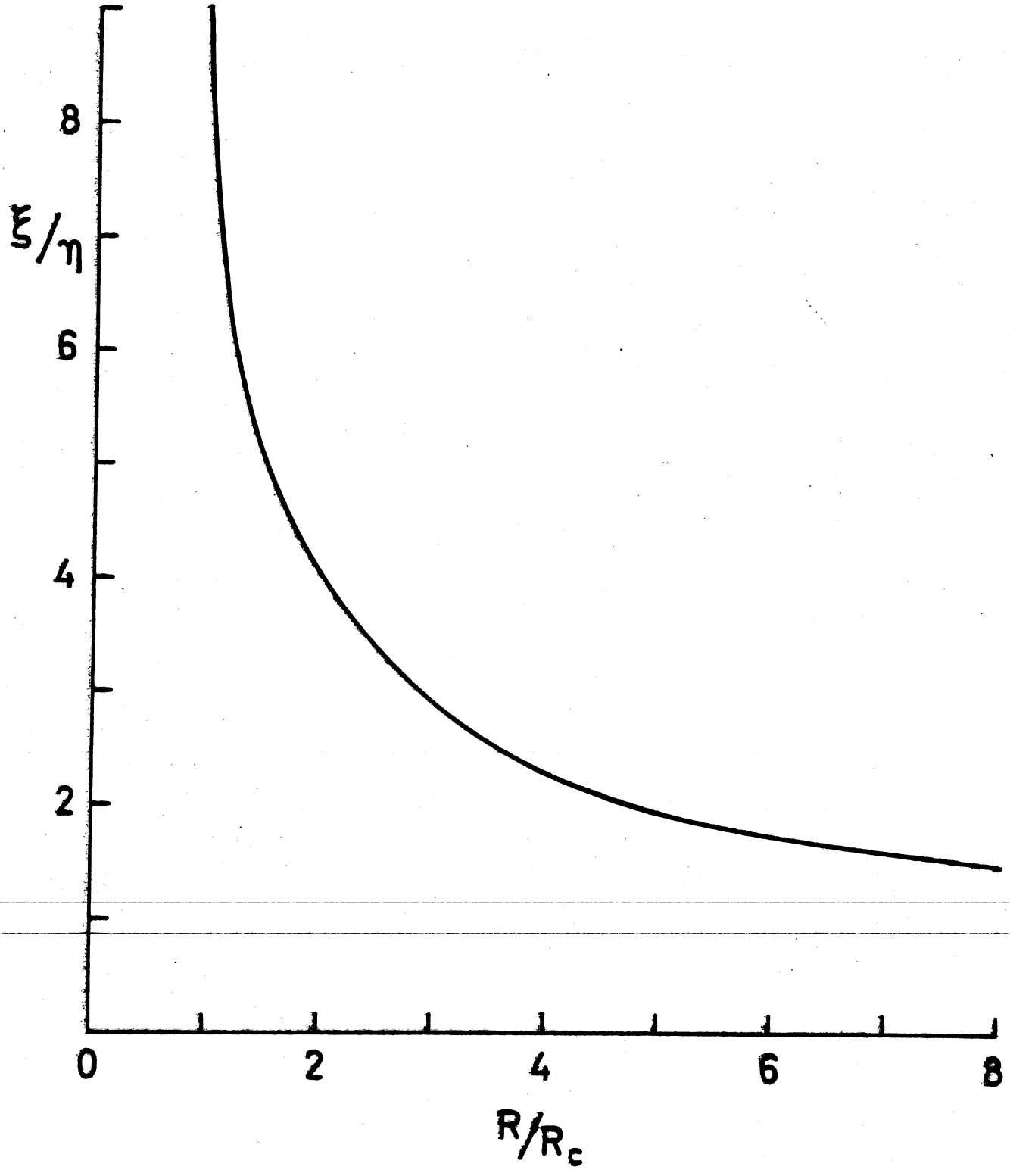

Fig. 6

Fig. 7

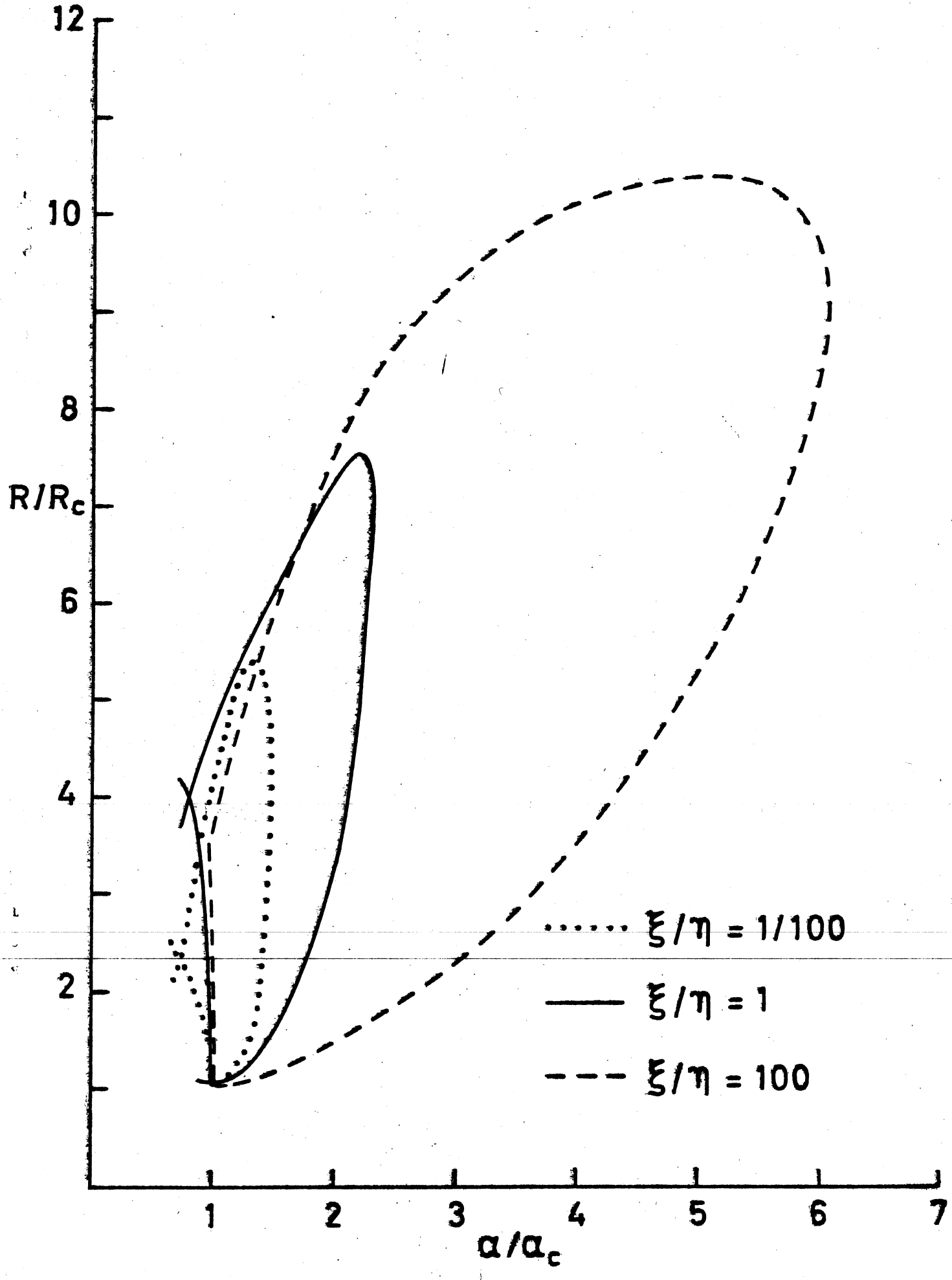

Fig. 8

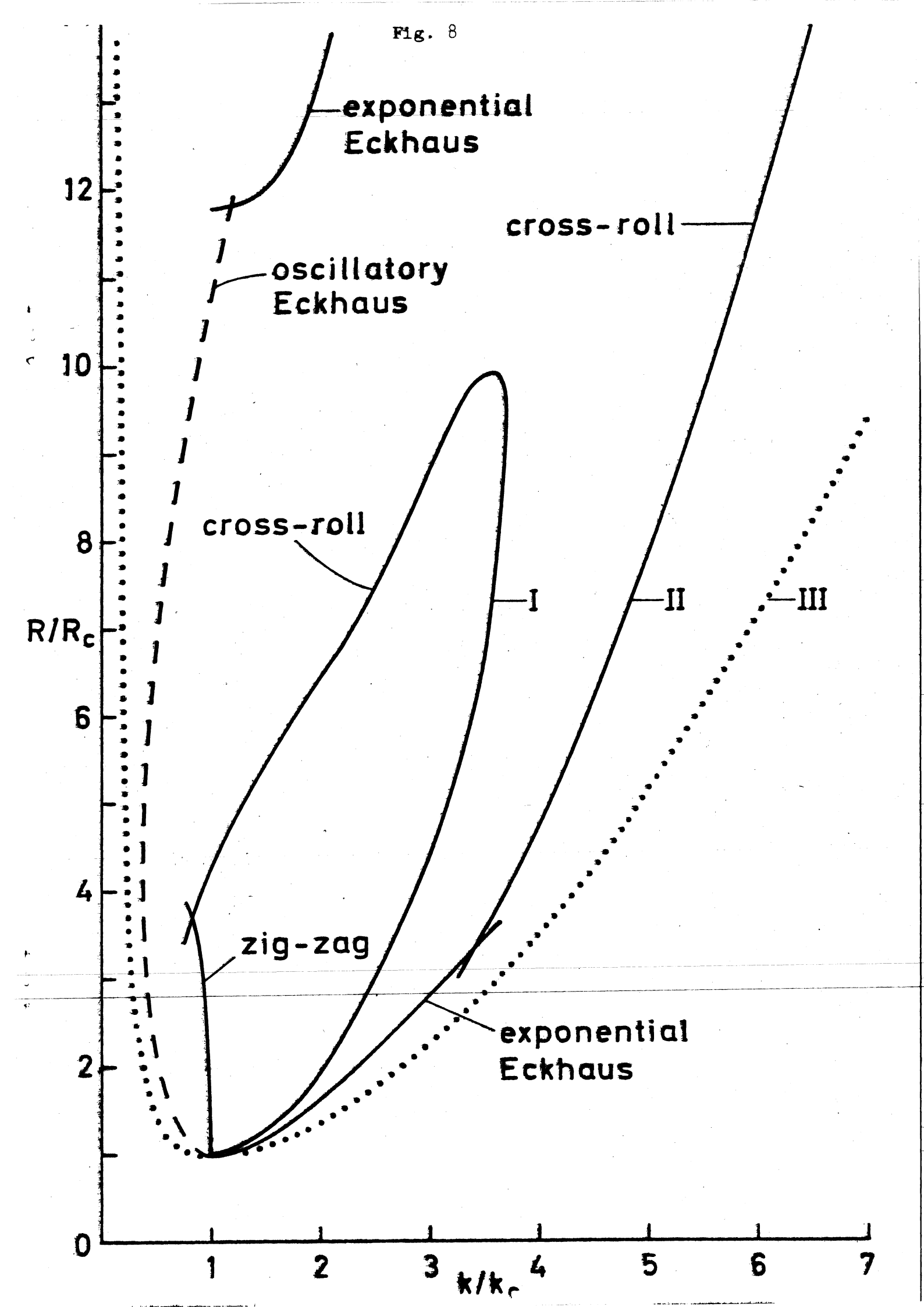
exponential
Eckhaus
cross-roll
oscillatory
Eckhaus
cross-roll
I
II
III
zig-zag
exponential
Eckhaus
R/Rc
k/kc
0
2
4
6
8
10
12
1
2
3
4
5
6
7

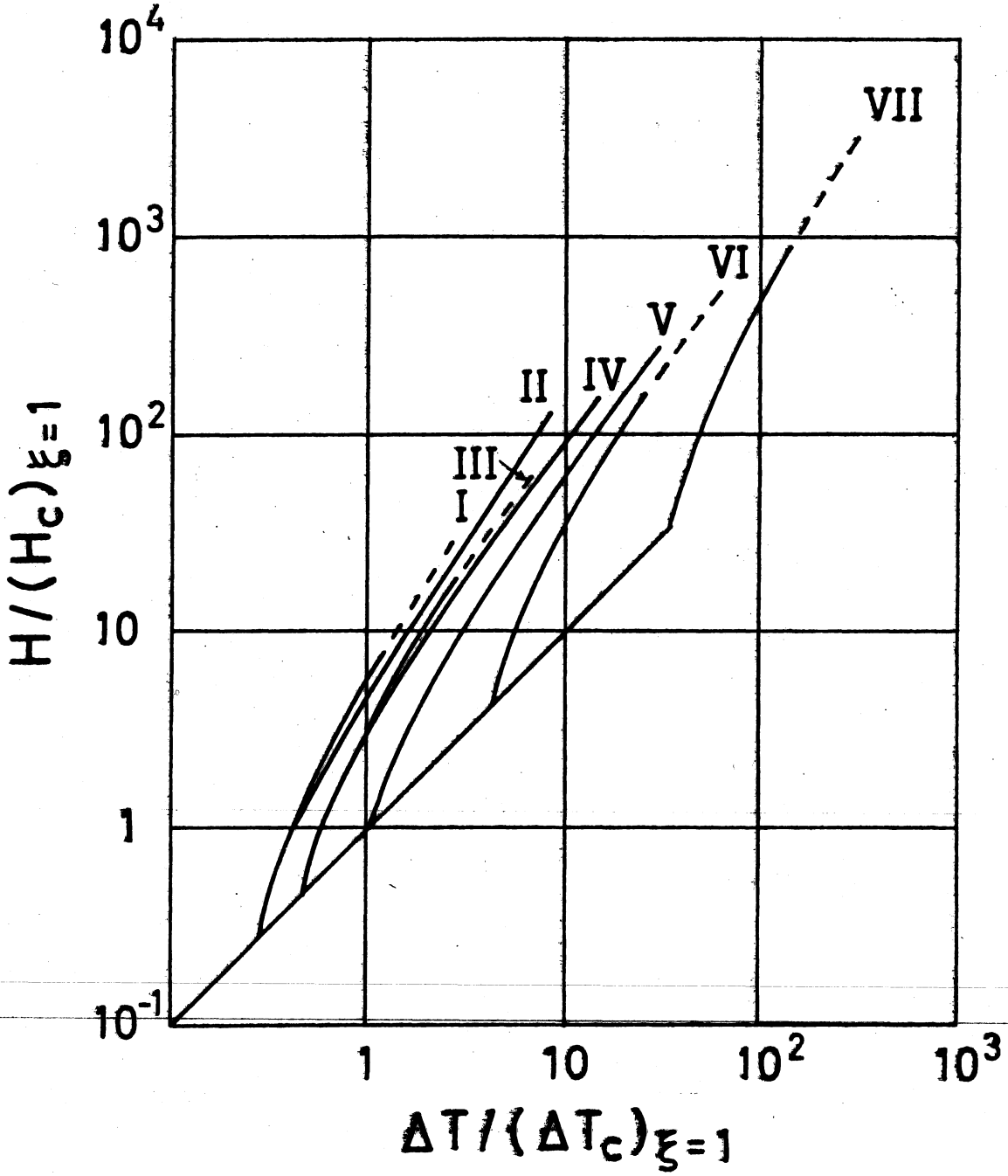
10^4
10^3
10^2
10
1
10^{-1}
$H/(H_c)_{\xi=1}$
VII
VI
V
IV
II
III
I
1
10
10^2
10^3
$\Delta T/(\Delta T_c)_{\xi=1}$

Fig. 9